Sensitivity of positron annihilation to plastic deformation

T. Wider, S. Hansen, U. Holzwarth, and K. Maier

Institut für Strahlen und Kernphysik der Universität Bonn, Nußallee 14-16, D-53115 Bonn, Germany

In situ measurements of the positron lifetime in copper single crystals during tensile tests and fatigue experiments have been performed. In tensile tests the mean positron lifetime starts to increase after a threshold value for the resolved plastic shear stress of $\tau \approx 10$ MPa has been exceeded. This stress, regarded as being a sensitivity threshold of positron annihilation to homogeneously distributed dislocations, belongs to a critical dislocation density of about 3×10^{12} m^{-2} and a mean dislocation spacing of about 0.5 μm. Since this spacing equals twice the mean diffusion length of positrons in copper ($L_+ \approx 0.25$ μm), positron annihilation is sensitive to dislocations when each positron has the chance of reaching a dislocation on its random walk. For deformations up to the threshold stress, positron trapping in vacancies produced by plastic deformation can be neglected. In fatigue, the positron lifetime starts to increase when a shear stress amplitude of $\hat{\tau} \approx 8$ MPa is exceeded. The corresponding inhomogeneous microstructure has been treated tentatively as a two-phase system consisting of dislocation-free (perfect crystal lattice) and densely populated (saturation trapping) areas. [S0163-1829(98)07509-2]

I. INTRODUCTION

Positron annihilation has proved to be a powerful tool in investigating the thermodynamical properties of vacancies in solids.[1–3] Since positrons are repelled by the positive ion cores in a solid, any interruption of the regular array of ion cores, in the simplest case a vacancy, can provide a positron trapping site. Analogously, dislocations are also expected to provide trapping sites. Indeed, it is generally observed that the mean positron lifetime increases with increasing plastic deformation (e.g., Refs. 4–8). Until now, the physical interaction mechanism between positrons and dislocations has been obscure[3,9,10] because it is covered by the many-sided aspects of the positron interactions with the complex defect spectra produced during plastic deformation.

While vacancies can exclusively be studied in a specimen in thermodynamical equilibrium at elevated temperatures, the formation of dislocations is always accompanied by the production of vacancies.[11–13] In addition, vacancies in thermodynamic equilibrium are homogeneously distributed whereas dislocations show a strong tendency to cluster with progressive deformation.[14–16] The formation of dislocation cells and peculiar dislocation arrangements, e.g., so-called persistent slip bands in fatigue[17,18] lead to a modulation of the dislocation density by a factor of $10^2 - 10^3$ on a typical length scale of 1 μm.[19–21] The dragging of jogs on dislocations with dominating screw character produces strings of vacancies,[11–13] which may disintegrate into stringlike clusters. For positrons trapped in these type of clusters lifetimes even shorter than those for single vacancies were calculated.[22] For large degrees of deformation and especially for fatigue, the annihilation of edge dislocations provides high concentrations of vacancies.[23] This mechanism favors a condensation of vacancies as Frank dislocation loops and the formation of spherical microvoids.[24,25] In fatigue, long-lived contributions (250–400 ps) are reported which are attributed to annihilation in spherical microvoids.[25–27]

In tensile experiments at least up to moderate plastic de-

formations of about 20%, the contributions attributed to vacancies and dislocations can be separated by careful annealing (e.g., Refs. 5 and 28) since vacancies are mobile and move to sinks (such as surfaces, grain boundaries, and dislocations) at temperatures lower than those required for recrystallization. Annealing experiments after plastic deformation of pure face-centered cubic metals show that vacancies produced during plastic deformation account for only a minor portion of the change in the mean positron lifetime.[29,30] The mean positron lifetime measured immediately after plastic deformation contains lifetime components from a confusing variety of possible trapping sites, among them different types of dislocations, vacancy condensates of different size and shape. The development of the mean positron lifetime during plastic deformation may therefore be influenced both by changes in the nature and concentration of positron traps. Experimentally, in most cases only the lifetime in the ideal lattice and a mean lifetime for deformation induced defects can be resolved.[28] Even after careful annealing great care has to be exercised when attempting to attribute a positron lifetime to a dislocation since the details of positron trapping along a dislocation line are probably impossible to control experimentally.

The ideal scenario for determining the specific lifetime and trapping rate in dislocations would be the use of a crystal free of vacancies that contains exclusively straight, undissociated, well-separated dislocations of either edge or screw character which do not contain jogs or kinks. Unfortunately, this scenario cannot be attained even in an approximate manner. In real crystals, dislocations stretch from one surface or grain boundary to another, either ending at dislocation nodes in the volume or forming closed loops consequently having different characters. Most attempts at determining the specific lifetime of positrons trapped in dislocations yield values close or slightly below the vacancy lifetime.[6,31,32] From this, it can be concluded that the positron lifetime may be related to vacancies trapped in the stress field around a dislocation line or in vacancies on a dislocation line which would be

equivalent to a pair of monoatomic jogs.[32]

The trapping rate into dislocations per unit dislocation concentration is found to range from 2×10^{15} s^{-1} (Ref. 28) to 2.9×10^{15} s^{-1} (Refs. 6,33) up to $1.6-3.5 \times 10^{16}$ s^{-1} (Ref. 34) which is significantly higher than the typical trapping rate per unit vacancy concentration in the range between $(4.3 \pm 0.8) \times 10^{14}$ s^{-1} (Ref. 35) and 9×10^{14} s^{-1}.[36] Temperature dependent positron annihilation measurements in the range between 10 and 300 K show that a dislocation line itself exhibits only a shallow positron trapping potential between 5–10 meV (Refs. 30, 37, and 38) and 30–40 meV.[5,10,39] The high specific trapping rate may then be explained by assuming trapping in a dislocation line as a precursor state for a transition into deeper traps such as jogs[5,38,40] or vacancies trapped in the stress field around a dislocation line.[41–43] Some support has been provided by theoretical calculations, which show that the extension of the trapping potential along the dislocation line will cause the wave function of the trapped positron to be similarly extended.[6] Additionally, the extension of the potential along the dislocation line leads to a quasicontinuum of bound states even for small binding energies.[6,44] Contrary to this, for vacancies, bound states can only exist if the potential V_0 is sufficiently deep to fulfill the condition $a\sqrt{2mV_0/h^2} > \pi/2$ where m denotes the positron mass and a is the radius of the vacancy assuming a spherical potential well.[6,45] Hence, it is concluded that the dislocation line may act as a trapping entity. Annihilation, however, takes place in other defects that are somehow associated with the dislocation line.

In order to throw some light on the trapping behavior of positrons in dislocations theoretical calculations have proved useful. Early calculations were based on the model of a hollow dislocation core and yielded excessively large binding energies between positrons and dislocations of a few eV.[46] This implied that the picture of a positron trapped in the dilatational zone around a text book edge dislocation was too simple. The model neglects details of the atomistic structure of the dislocation core due to dissociation into partial dislocations, relaxation effects in the stacking fault ribbons between the partials, and the existence of jogs. Recent molecular dynamic simulations yielded values in the range of 40 to 100 meV for direct positron trapping in dislocation lines.[41,47] These calculations confirm a possible trapping of positrons in jogs and vacancies associated with a dislocation line and yield positron lifetimes which are compatible with the experimentally observed lifetimes, but which are a little shorter than those for vacancies.[41] The calculations of Manienen et al.[41] also agree with earlier theoretical treatments by Martin and Paetsch,[48] thus indicating that annihilation at dislocations should yield very nearly the same lifetime as that in the bulk material.

In spite of this unsatisfactory situation, many positron-annihilation investigations demonstrate the usefulness of the method in detecting microstructural evolution during creep,[49] fatigue,[26,50–52] thermofatigue,[53] and precipitation phenomena.[54] Therefore, it seems promising to give thought to a possible application of positron annihilation, as a complementary tool, to nondestructive testing. For an evaluation of the potential of the method further systematic investigations are required to reveal the behavior of positrons in the complex microstructures of plastically deformed materials.

Experimental investigations are cumbersome since several methods have to be combined to characterize the main features of the defect spectra produced by plastic deformation. Although transmission electron microscopy (TEM) is an excellent tool for studying dislocation arrangements and dissociation into partials, single vacancies and clusters remain invisible with the exception of large Frank loops and sperical clusters exceeding a diameter of approximately 1 nm. Electrical resistivity measurements, on the other hand, are higly sensitive to all defects either visible or invisible to TEM, but are not at all specific. For metals, no techniques are available for specifically observing monoatomic jogs on dislocations and vacancies elastically bound to them. Thus, any systematic investigation of the positron-dislocation interaction will be an iterative process; the information partly delivered by positron annihilation. *In situ* positron annihilation measurements should be performed in order to follow the microstructural evolution in one specimen and to avoid sectioning or the simultaneous identical deformation of two specimens as required by the sandwich technique. This would allow the use of a larger number of specimens to critically check the reproducibility of the measurements. In order to keep the defect spectra as simple as possible special attention should be paid to the early stages of deformation and preferably single crystals oriented for single slip should be used. A lot of time can be saved by choosing materials (e.g., pure copper or nickel) whose microstructural evolution has already been thoroughly investigated both by TEM and by electrical resistivity measurements for various deformation conditions.

The present paper deals with *in situ* positron lifetime measurements performed with a β^+-γ spectrometer[55] on copper single crystals during tensile deformation and symmetric push-pull fatigue. The *in situ* technique permits to investigate the microstructural evolution during plastic deformation on a single specimen. The experimental details are outlined in Sec. II. The most important result, presented in Sec. III, concerns the existence of threshold stresses of about 10 and 8 MPa which have to be exceeded before the mean positron lifetime starts to increase during tensile deformation and fatigue, respectively. In Secs IV A and IV B an attempt is made to interpret the tensile and fatigue threshold stresses in relation to the different microstructures. Finally, some considerations for the trapping mechanism of positrons into dislocations are given in Sec. IV D. The central experimental findings and the conclusions are summarized in Sec. V.

II. EXPERIMENTAL PROCEDURE

A. Specimen preparation

The tensile test and fatigue experiments were performed on copper single crystals oriented for single slip with crystallographic orientation factors μ close to 0.5. The crystals were grown in a graphite crucible by the Bridgman technique at the Max-Planck-Institut für Metallforschung in Stuttgart. The crystals were cylindrically shaped, about 50 mm long and had a diameter of 5 mm. In the center a gauge length of $l_0 = 10$ mm with a reduced diameter of 4.5 mm was prepared by spark erosion. The damaged surface was removed by an

electrolytical polish leaving a final diameter of 4.0 mm. Finally, the orientation factor μ was determined from a Laue diffractogram taken on the polished surface.

B. Plastic deformation

In order to facilitate *in situ* positron annihilation measurements and comparison with available investigations of the microstructural evolution during deformation, tensile tests and symmetric push-pull deformations of cylindrical specimens were chosen. Cold rolling is often applied because it easily delivers flat specimens easily for use in the sandwich technique. *In situ* positron annihilation is, however, difficult to perform in this case and the very early stages of deformation with simple dislocation structures are difficult to control. In a more advanced phase of the investigation we plan to perform in-beam experiments with an intense high energetic positron beam at an accelerator facility, therefore a deformation machine was constructed to precisely meet future size requirements.

All plastic deformation experiments were performed under strain control in a closed-loop controlled machine for the tensile and fatigue experiments. The machine is driven by a highly sensitive piezoelectric translator,[56] capable of a maximum extension of 180 μm at an applied voltage of 1.000 V and a maximum force of 4.500 N. Due to the limitations of the piezoelectric translator the load frame (size about 240 mm $\times$ 500 mm) was designed to be extremely stiff in order to avoid that the plastic deformation of the specimen is accompanied by a measurable elastic deformation of the machine components. The load cell was manufactured in our laboratory to meet exactly the required force resolution of 0.5 N. Although commercially available ones are known to have better resolutions they are elastically too soft. The load cell consisted essentially of a phosphorous bronze tube (diameters: outside 30 mm, inside 19 mm) whose thick walls were reduced to 0.5 mm thickness over a length of 15 mm. The deformation of the tube, being purely elastic under the given conditions, was measured with four strain gauges, forming part of a Wheatstone bridge. The load cell was calibrated with reference weights and the linearity ($\leq 0.1\%$) and reproducibility ($\leq 0.1\%$) were checked up to 1.500 N.

The strain was measured with a capacitance strain transducer.[57] The capacitor plates were fixed sideways on the specimen grips and were adjusted at a distance of 300 μm parallel to each other, which resulted in a capacity of 3.3 pF. A resolution of about 0.1 μm was achieved. Figure 1 outlines the mechanical setup for the deformation experiments.

The experiments were run with a triangular command wave for the total strain, generated by a PC at frequencies in the range between 0.2 and 2.0 Hz. The frequency is not a crucial parameter in the experiments since the strain-rate sensitivity of face-centered cubic metals is very small.[58] The force F and the extension Δl of the specimens were recorded during the experiments. The stress $\sigma = F/A$ and the total strain $\epsilon = \Delta l/l_0$ were then calculated, where A denotes the cross section of the specimen. By making use of the crystallographic orientation factor μ, the shear stress $\tau = \mu\sigma$ and the shear strain $\gamma = \epsilon/\mu$ both resolved to the primary glide plane were obtained.[59]

For the tensile tests, hardening curves, i.e., curves of the resolved shear stress τ versus resolved shear strain γ, were
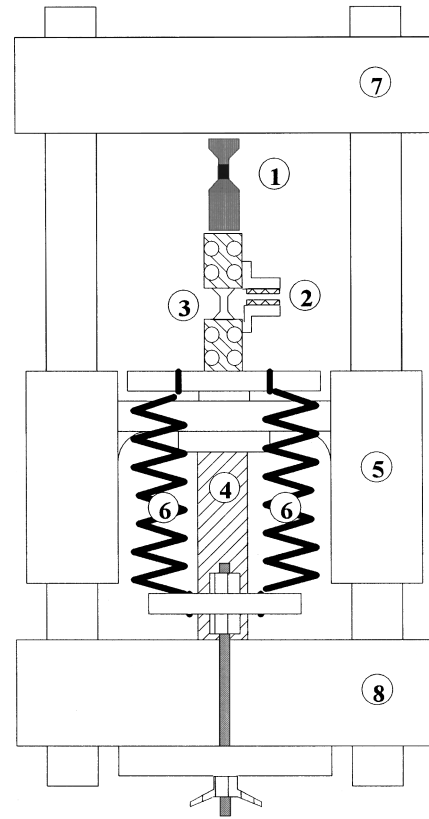

FIG. 1. Sketch of the (cyclic) deformation machine. Load and elongation are measured by the load cell (1) and the capacitance strain transducer (2), respectively. The specimen is held by upper and lower grips (3). The elongation of the piezo element (4) causes a compression of the specimen. Since the piezo element can only exert a compressive force, tensile forces are provided by the stretched springs (6). The movable part (5) assures coaxiality and avoids shear stresses on the piezo element which might easily destroy it. The upper and lower cross heads are represented by (7) and (8).

recorded. For the fatigue tests, τ versus γ yields hysteresis loops. The size of the loops is given by the amplitude of the resolved total strain $\hat{\gamma}$ and the respective amplitude of the resolved shear stress $\hat{\tau}$. The resolved plastic strain amplitude $\hat{\gamma}_{pl}$ is obtained from the opening of the hysteresis loops at zero force. In the fatigue experiments, the hysteresis loops usually change their shape and size due to the effects of cyclic hardening or softening. Thus, cyclic hardening curves, i.e., plots of the resolved shear stress amplitudes $\hat{\tau}$ versus the cumulative plastic strain $\gamma_{cum} = 4N_i\hat{\gamma}_{pl,i}$ provide an adequate representation (see Ref. 60). Here, N_i denotes the number of fatigue cycles carried out with an amplitude $\hat{\gamma}_{pl,i}$.

C. *In situ* positron annihilation measurements

The applied positron annihilation technique which has been developed for *in situ* lifetime measurements has already been described in detail elsewhere.[55] The most important ideas will be outlined below.

A β^+-γ spectrometer was used instead of a γ-γ spectrometer in order to obtain higher coincidence counting rates. For this purpose, a ^{72}Se/^{72}As generator was vapor deposited in a hole of 0.6 mm (internal diameter) in a gold collimator of 2
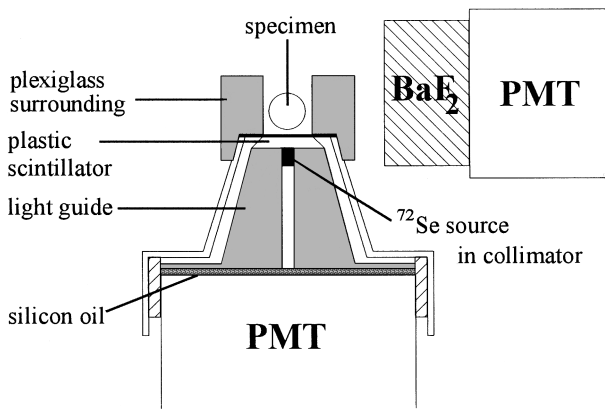
FIG. 2. The β^+-γ-coincidence spectrometer. The ^{72}Se/^{72}As source in the gold collimator is integrated in a plexiglass light guide on a photomultiplier tube (PMT: Philips XP 2020) and covered by a thin plastic scintillator that provides the start signal. The γ quanta are detected by a 1.5 in. BaF$_2$ detector. In order to catch the major part of the positrons missing the copper specimen or being reflected by its surface, it is surrounded by plexiglass. Details have been published in Ref. 55.

mm (external diameter). This collimator was covered by a thin (1 mm) plastic scintillator and was placed in front of the specimen. The positrons, which are emitted in the direction towards the specimen, lost on average about 150 keV of their kinetic energy in the plastic scintillator and created the start signals for the lifetime measurement. Positrons which annihilated in the gold collimator or in the source itself did not provide a start signal, which appreciably reduces the background. The experimental setup is depicted in Fig. 2.

The copper specimens were surrounded by plexiglass which absorbs the positrons that miss the copper specimen or that are reflected by its surface. In plexiglass and in the plastic scintillator positronium is formed whose much longer lifetime of about 1.200 ps (pick-off annihilation) is clearly discernible from the 100 to 200 ps expected for a deformed metal. The contribution of positrons annihilating in the plexiglass and the plastic scintillator can, therefore, be corrected by a weighted subtraction of a plexiglass reference spectrum. A deconvolution of the spectra with an apparative resolution function was not performed, i.e., the lifetimes presented in the next section were obtained from a least square fit of a single exponential function. The constant contribution of the apparative resolution to the mean lifetime is only noticeable for short values. Therefore, the bulk lifetime of copper was found to be about 20 ps longer than the generally accepted value of 110 ps (Ref. 71) whereas the 175 ps found in fatigued specimen were in fair agreement with other measurements.[8,73] The observed increase of the mean lifetime with progressing deformation is smaller than that expected from a full fitting procedure but this is not a limitation for determining a sensitivity threshold.

The ^{72}Se/^{72}As generator provides two positron spectra with maximum energies of up to 2.5 and 3.3 MeV and a prompt γ quantum of 835 keV. Even after the loss of 150 keV in the start scintillator, the largest part of the positrons thermalizes at least 250 or 400 μm below the surface for the two spectra, respectively. This is large enough to assess real bulk properties. The prompt γ quantum can be used for an

on-line measurement of the time resolution of the spectrometer. A value of 280 ps was obtained.[55]

This technique permits us to follow the cyclic hardening curve by *in situ* lifetime measurements. There was no need to stop the fatigue experiments for the lifetime measurements since the microstructural evolution yielded only small changes during the few minutes required to record a lifetime spectrum containing 10^6 annihilation events. For the tensile tests, the deformation was stopped with load applied for the lifetime measurements; stress relaxations due to slight rearrangements of the dislocations being allowed. In order to achieve large plastic deformations, when the maximum extension capacity of the piezo translator was exhausted, the specimen had to be dismounted in the position of maximum tensile strain and had to be remounted after the piezo translator had been repositioned to zero. This procedure had no detectable influence on the positron lifetimes. In this way, dozens of lifetime spectra were recorded which reflected the evolution of the microstructure in the specimens under examination. In contrast, the sandwich technique, which requires two identical specimens cut from the same plastically deformed crystal, would require more than 150 single crystals to obtain the same information as that obtained from the tensile tests presented in the following section, and several hundred for the fatigue experiments.

The evaluation of the positron data was restricted to the mean positron lifetime. Since our *in situ* measurements were performed at room temperature and without the possibility of an additional *in situ* annealing it is for example impossible to distinguish between positrons annihilating in vacancies in the lattice and in vacancies associated with dislocations. Moreover, according to literature, one may expect lifetimes of positrons annihilating in jogs to be unresolvably close to those annihilating in vacancies. The same holds for positrons annihilating in the perfect lattice and along the undisturbed dislocation line. Thus, no additional information would be gained in the present case and assumptions on defect-specific positron lifetimes would be needed which cannot be checked within the framework of the experiments presented here.

III. RESULTS

A. Tensile tests and fatigue

Six tensile tests and five fatigue experiments were performed on copper single crystals. In Fig. 3, two typical examples of the development of the mean positron lifetime ($1/\bar{\lambda}$) during tensile deformation of a copper single crystal are presented. In plasticity theory τ denotes a mechanical shear stress resolved to the primary glide plane. In order to avoid confusion with the positron lifetime, the inverse decay rate $1/\lambda$ is used. The magnitude of the error flags (± 2 ps) is determined by the scatter of repeated measurements at constant microstructure. The evaluation of the lifetime spectra should only account for a statistical error of ≤ 0.5 ps. In Fig. 3 the strain is given on a logarithmic scale in order to visualize possible lifetime changes in the microplastic region. It can easily be recognized that the specimens had to be deformed to at least $\gamma \approx 3\%$ before $1/\bar{\lambda}$ started to increase. Figure 3(a) shows the typical features observed in tensile test. The increase of the mean positron lifetime followed the increase of the shear stress with progressive hardening. No
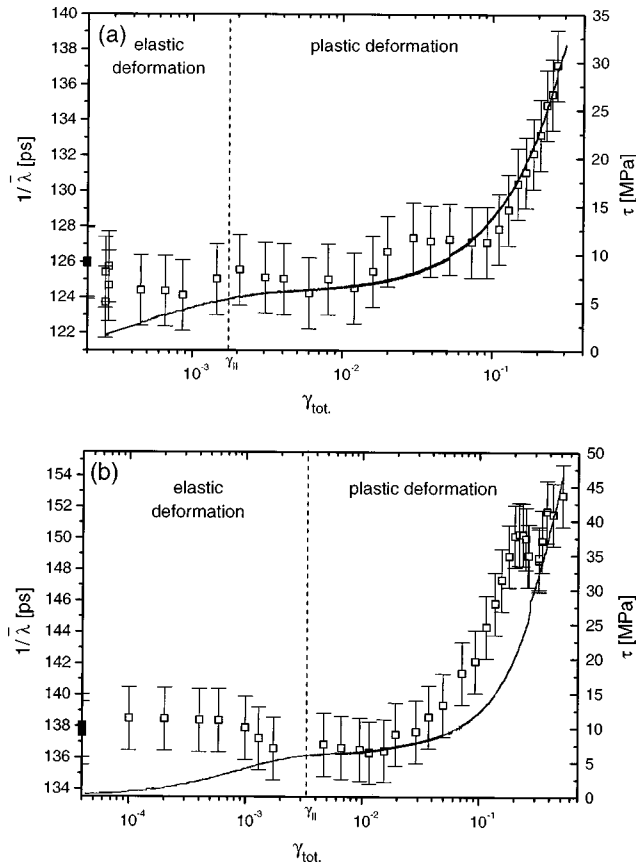
FIG. 3. Tensile hardening curves (line), and the development of the mean positron lifetime $1/\bar{\lambda}$ ($\square$) during two tensile tests as a function of the logarithm of the total resolved shear strain γ. The mean positron lifetime $1/\bar{\lambda}$ remains constant up to strains of 3% and resolved shear stresses of 10 MPa; (a) shows the typical behavior and (b) presents data from the only test (out of 6) showing a possible onset of saturation at a stress which is lower than in other specimens not showing this feature.

FIG. 4. Two typical cyclic hardening curves, shear stress amplitude $\hat{\tau}$ ($\bullet$) in MPa versus cumulative plastic strain γ_{cum} and the related mean positron lifetime $1/\bar{\lambda}$ ($\bigcirc$) in ps. $1/\bar{\lambda}$ increases from about 130 ps to a saturation value of about 170 to 175 ps. $\hat{\tau}$ saturates at around 30 MPa.

indication of a saturation in the mean positron lifetime up to 50% plastic strain and $\tau=43.5$ MPa is found. Deviating from the general findings, Fig. 3(b) suggests the onset of a saturationlike state at a resolved tensile shear stress of about 20 MPa. However, after further straining the positron lifetime seems to increase again. Such a behavior was not observed in any other specimen.

The fatigue experiments were performed as so-called multiple step tests, i.e., the applied amplitude $\hat{\gamma}$ was increased step by step after no further changes in the resolved shear stress amplitude $\hat{\tau}$ were measurable. The experiments were started with resolved plastic strain amplitudes in the range $2 \times 10^{-5} \leqslant \hat{\gamma}_{pl} \leqslant 2 \times 10^{-4}$. The maximum applied plastic strain amplitude was $\hat{\gamma}_{pl}=4 \times 10^{-3}$. Figure 4 presents two typical results. For the case of amplitudes below $\hat{\gamma}_{pl} \approx 1 \times 10^{-4}$, the mean positron lifetime $1/\bar{\lambda}$ started to increase if the shear stress amplitude $\hat{\tau}$ exceeded about 8 MPa. A tendency to saturate became obvious at around 25 MPa.

In Fig. 5 the mean positron lifetime is plotted versus the resolved shear stress of a copper single crystal deformed in tension for the two specimens presented in Fig. 3. The positron lifetime remains constant up to a threshold stress and then starts to linearly increase with the resolved shear stress.
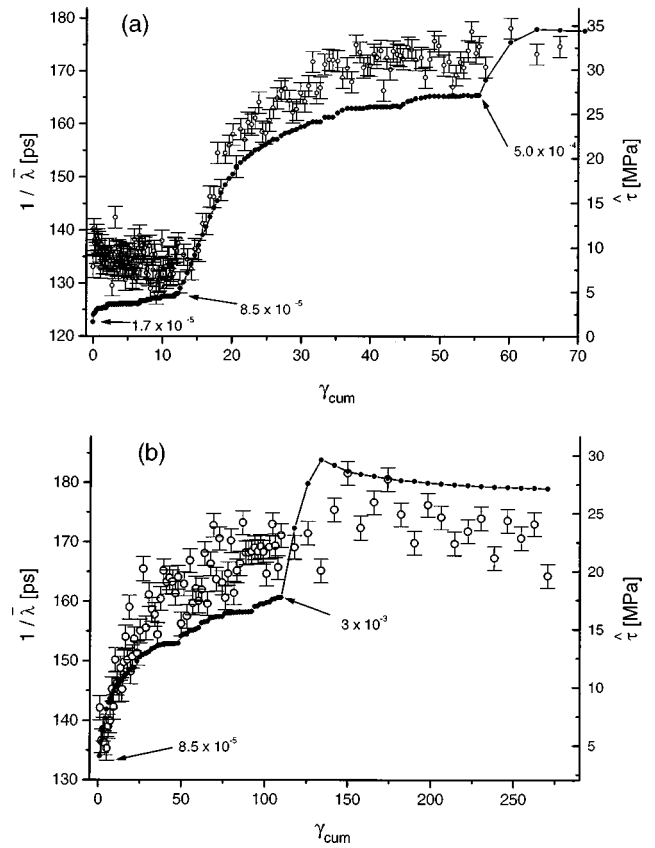
The threshold stresses derived from the intersection of the dashed lines (linear regression fits) are remarkably reproducible; a value of (10 ± 1) MPa is obtained for tensile deformation. The same feature is observed in fatigue as can be recognized by Fig. 6 where the positron lifetime is plotted versus the shear stress amplitude. The threshold stress which has to be exceeded in fatigue before the mean positron lifetime increases was obtained as (8 ± 1) MPa. Between the threshold stress and the lifetime saturation which sets in at about 25 MPa the dependence of the positron lifetime on the shear stress amplitude may be approximated by a linear increase, in spite of the scatter.

Whereas the slope in the linearly increasing part of Fig. 5 was approximately constant (0.8 ps/MPa) in tensile tests, the respective slopes determined from fatigue experiments (Fig. 7) showed a tendency to decrease with increasing applied plastic shear strain amplitude $\hat{\gamma}_{pl}$. In the framework of this consideration, a tensile test may be regarded as a fatigue experiment with infinite amplitude, i.e., the virgin curve of the first hysteresis is ''never'' finished. Indeed, the slopes obtained from typical $1/\bar{\lambda}$ versus τ plots of the tensile experiments yield the smallest determined values of about 0.8 ps/MPa.

B. Annealing after plastic deformation

The results of the mean positron lifetimes after a two stage annealing treatment on a single crystal after tensile
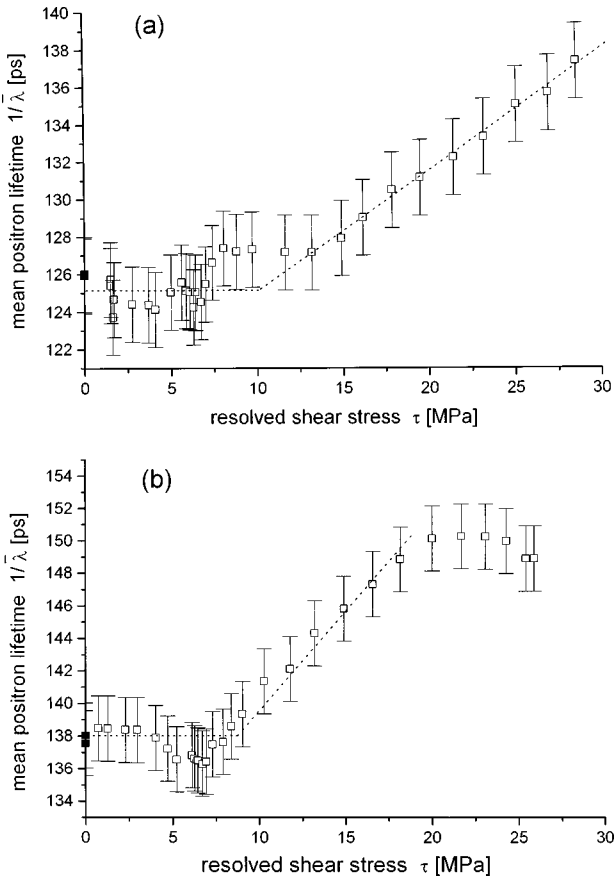
FIG. 5. Plot of the mean positron lifetime $1/\bar{\lambda}$ versus the resolved shear stress τ for tensile tests; (a) and (b) correspond to the respective plots in Fig. 3. From the intersection points of the dashed lines (linear regression fits) threshold stresses of (10 ± 1) MPa were derived. Above the threshold stress the positron lifetime increases linearly with the resolved shear stress. The saturationlike behavior in (b) has only been observed in this specimen. A comparison with (a) shows that typically the positron lifetime $1/\bar{\lambda}$ continues to increase up to the maximum stresses between 30 and 43.5 MPa reached in the experiments.
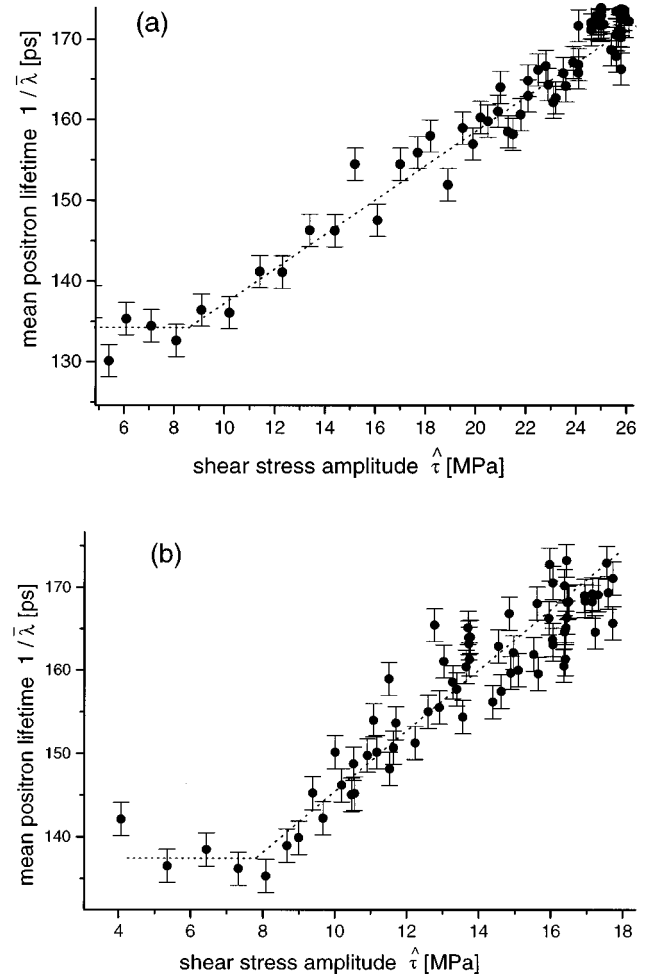

FIG. 6. Plot of the mean positron lifetime $1/\bar{\lambda}$ versus the resolved shear stress amplitudes $\hat{\tau}$ for the fatigue tests presented in Fig. 4. Threshold stresses of (8 ± 1) MPa are observed. In spite of the scatter of the data a linear increase of $1/\bar{\lambda}$ with increasing $\hat{\tau}$ describes the experimental findings between the threshold and the saturation stress of about 25 MPa.
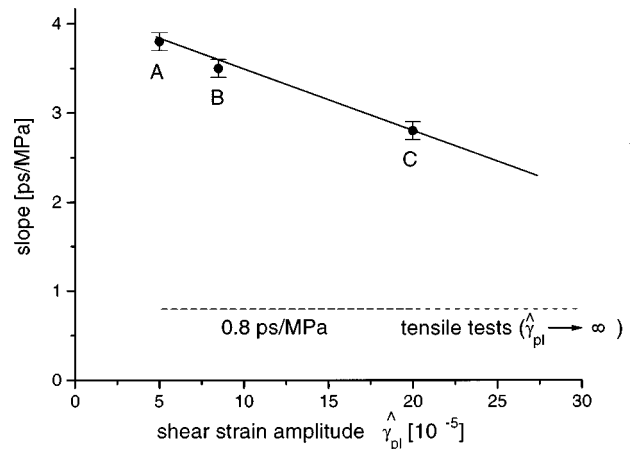

FIG. 7. The slopes determined by a linear regression fit from diagrams such as those in Fig. 6(b) depend systematically on the applied resolved plastic strain amplitude $\hat{\gamma}_{pl}$. The line offers only an eye guide. The mean value of $d(1/\bar{\lambda})/d\tau$ for infinite $\hat{\gamma}_{pl}$ taken from the tensile tests is indicated by the dotted line.

deformation to $\gamma = 50\%$ and $\tau = 43.5$ MPa and on a crystal fatigued in a multiple step test to a flow stress amplitude in cyclic saturation of about $\hat{\tau}_{sat} = 34$ MPa after a cumulative plastic strain of $\gamma_{cum} \approx 70$ are tabulated in Table I. For ease of comparison the change of the mean positron lifetime is given. After deformation, the crystals were stored at room temperature for about four weeks. Before the two-stage annealing treatment, the positron lifetime was measured again and no significant change was observed. The crystals were then subjected to a temperature of 450 K in the first stage and to 550 K in the second stage, for 60 min, respectively. The annealing was performed under vacuum at $p \leqslant 10^{-3}$ Pa. The temperatures were chosen to be below the recrystallization temperature in order to avoid noticeable changes in the mesoscopic dislocation arrangement.

Although the resolved shear stress reached by tensile deformation is much higher than the resolved shear stress amplitude in the state of cyclic saturation in fatigue, the increase in the mean positron lifetime is more than twice as large. Additionally, the defect spectra in the fatigued crystal are more resistant to annealing than those created in the tensile

TABLE I. The change of the mean positron lifetime in copper single crystals with respect to the undeformed state after tensile deformation ($\gamma=0.5$, $\dot{\gamma}=1\times10^{-4}$ s^{-1}, $\tau=45$ MPa), after fatigue ($\hat{\tau}_{\text{sat}}\approx34$ MPa, $\hat{\gamma}=5\times10^{-4}$, $\gamma_{\text{cum}}=70$) and after different successive annealing stages.

Treatment	Change of mean positron lifetime	
	Tensile test	Fatigue
After plastic deformation	(16 ± 2) ps	(39 ± 2) ps
After 4 weeks at 293 K	(16 ± 2) ps	(39 ± 2) ps
After 60 min at 450 K	(8 ± 2) ps	(31 ± 2) ps
After 60 min at 550 K	(8 ± 2) ps	(25 ± 2) ps

specimen. In the first stage of the annealing treatment, all defects which can anneal before recrystallization occurs are eliminated and only 50% of the increase in positron lifetime is retained. The annealing of the fatigue specimen occurs gradually and 65% of the increase in the positron lifetime is retained.

IV. DISCUSSION

Applying the *in situ* technique[55] outlined in Sec. II, about 30 lifetime spectra were recorded during the deformation of each tensile specimen. Thus, the evolution of the microstructure could be studied in a single specimen. Other crystals were used to critically check the reproducibility. The most striking finding was a threshold stress for the increase of the mean positron lifetime that may be interpreted as the sensitivity limit of positron annihilation to dislocations. This will further be discussed in Sec. IV A.

Such a threshold was also observed for the fatigue experiments. Although the main features of a plot of the mean positron lifetime versus the resolved tensile shear stress (see Fig. 5) or the resolved shear stress amplitude (see Fig. 6) appear to be identical, their interpretation must take into account microstructural differences.

Copper was chosen because it has been carefully investigated by electron microscopy during all stages of unidirectional and cyclic deformation. Thus, the literature could be consulted for reliable dislocation density and distribution data.[14–16,19–21]

A. Tensile deformation

1. Dislocation density and distribution

A comparison of the hardening curves obtained experimentally with those typically obtained from tensile tests on single crystalline face-centered cubic (fcc) metals (e.g., Refs 16 and 61) shows that the threshold stress of about (10 ± 1) MPa lies in stage II of the hardening curve. The resolved shear stress τ can be related to the dislocation density ϱ via the relation[42,61]

$$\tau=\alpha b G \sqrt{\varrho}, \qquad (1)$$

where α is a numerical factor in the range $0.3\leqslant\alpha\leqslant0.5$.[42,61,62] b denotes the modulus of the Burgers vector and G the shear modulus. The validity of Eq. (1) has been confirmed experimentally by several authors (e.g., Refs. 15 and 63). The

equation permits the interpretation of the threshold stress in terms of a critical dislocation density. With $b=2.56\times10^{-10}$ m (Ref. 64), $G=42.100$ MPa (Ref. 65) and setting $\alpha=0.5$ a critical dislocation density of $\varrho_c=(3\pm1)\times10^{12}$ m^{-2} is obtained.

In order to draw further conclusions the spatial distribution of these dislocations has to be considered. A homogeneous distribution would imply that each thermalized positron has statistically an equivalent environment.

It is known from TEM that dislocations show a tendency to cluster and to form dislocation dipoles during tensile deformation.[14–16] From micrographs of copper single crystals after tensile straining to about 6 and 16 MPa at 293 K,[14] it can be concluded that the dislocation arrangement at 6 MPa can be regarded as homogeneous apart from a few dipoles. At 16 MPa the homogeneous distribution is disturbed by primary edge dislocation dipoles, some of them being arranged in groups. From these micrographs it can be concluded that at 10 MPa the picture of a homogeneous distribution of dislocations is a tenable approximation. Thus, we may consider positrons as diffusing particles in a system of homogeneously distributed single dislocations having an average separation of $d=1/\sqrt{\varrho_c}\approx0.5$ μm.

2. The role of vacancies—concentration and distribution

Subsequently, it will be shown that the concentration of vacancies produced during plastic deformation is not the proper quantity to describe their possible contribution to the increase in the mean positron lifetime. While vacancy formation in thermal equilibrium yields a homogeneous distribution in a crystal, plastic deformation produces vacancies arranged in strings.

The most important production mechanism for vacancies and interstitials is the dragging of nonglissile jogs on moving dislocations with dominating screw character.[11–13] Jogs are created by the intersection of so-called forest dislocations with gliding dislocations. Forest dislocations belong to secondary glide systems. They are inclined to the primary glide plane and impede the motion of primary dislocations. A nonglissile jog on a gliding screw dislocation will impede its further motion. As these jogs are forced to climb by the gliding dislocation, atomic defects are produced. Depending on the direction of dislocation motion a nonglissile jog leaves behind in its wake a string of vacancies or interstitials. The situation is depicted in Fig. 8. Due to the low number of edge dislocation dipoles the production of atomic defects by collapsing narrow dipoles (dislocation annihilation) can be neglected in the early stage II of the hardening curve.

An initially homogeneous dislocation distribution, as in our case, will also cause the intersection jogs and consequently the strings of atomic defects to be homogeneously distributed. Since a direct measurement of the absolute vacancy concentration is not possible we have to rely on theoretical calculations for the production of atomic defects. As the mean positron lifetime at the threshold stress is just exceeding the statistical scatter, the vacancy contribution to the increase of the mean positron lifetime cannot be determined by annealing experiments.

A quantitative approach conceived by Saada[62] yields a vacancy concentration
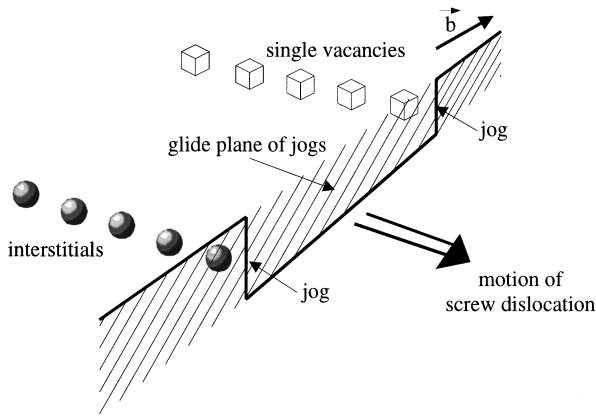
FIG. 8. A screw dislocation contains two jogs which may originate from two intersection processes with forest dislocations. These jogs are glissile only along the dislocation line (hatched plane). In this way, they can annihilate. If we assume that no annihilation occurs, they are forced to move together with the screw dislocation in the direction indicated. The jogs have to leave their glide plane by climbing. Thus, the traces of the jogs are marked by strings of interstitials and vacancies (Refs. 11–13).

$$C_V = \frac{1}{2} \frac{\beta}{G} \int_0^\gamma \tau \, d\gamma. \qquad (2)$$

β is a numerical constant which can be determined from electrical resistivity measurements or calorimetric measurements of the stored energy and G denotes the shear modulus. The integral determines the mechanical work done to the crystal. The factor $\frac{1}{2}$ has been introduced because interstitials and vacancies are produced in equal concentrations. Values of β have been compiled by van den Beukel.[66] With an average value of $\beta=0.06$, $\gamma \approx 3\%$, and $\tau \approx 10$ MPa a vacancy concentration of $C_V \approx 2 \times 10^{-7}$ is calculated. It needs to be emphasized that although this concentration is equivalent to the sensitivity limit of positron annihilation to vacancies in thermodynamical equilibrium,[3] vacancies cannot be responsible for the plastic deformation threshold obtained. The different spatial distribution of vacancies in thermodynamical equilibrium and produced by plastic deformation cause some important differences: (i) strings are more difficult to find for diffusing positrons than the same amount of homogeneously distributed vacancies; (ii) calculations by Corbel et al.[22] indicate that the disintegration of vacancy strings into string-like clusters yields positron lifetimes which may be shorter than those for single vacancies; and (iii) the physical interpretation given by van den Beukel[66] is that of vacancy strings with a total length of 5–10 % of the dislocation length in m/m^3. These strings can be imagined as little twigs attached to branches, i.e., dislocations. The twigs are invisible by TEM as they are not surrounded by far reaching stress fields like dislocations. Keeping in mind that the specific trapping rate for dislocations is significantly higher than that for vacancies,[6,28,33] the probability of being trapped by a dislocation is 10 or 20 times higher than that of being trapped in a vacancy. Finally, the annealing experiments indicate that a spatial redistribution of vacancies need not be considered due to their low mobility at room temperature.

Assuming that a positron once trapped neither escapes from a dislocation (see Sec. IV D) nor from a vacancy string

and that the positron is trapped at the dislocation or vacancy string that it reaches first, then both the dislocations and vacancy strings may be treated as linear defects with a total density of $(3 \pm 1) \times 10^{12}$ m^{-2} plus a 5–10 % correction due to the total length of vacancy strings. Provided that the specific lifetimes of positrons trapped in vacancy strings and dislocations are not too different, the small amount of positrons trapped in vacancy strings will not significantly influence the mean positron lifetime.

In order to check possible differences in the positron lifetimes, we have to consider the effects of rearrangements of the strings, for example segmentation or formation of spherical vacancy clusters. Calculations of the positron lifetime in sperical vacancy clusters usually show strongly increasing lifetimes with increasing void radii.[67] For divacancies in copper, lifetimes of 250 ps are reported.[68] On the other hand calculations by Corbel et al.[22] show that the positron lifetime always decreases if the relaxation processes for the nearest neighboring atoms are taken into account. The relaxed configuration may result in a positron lifetime that is shorter than that in a monovacancy.[22] Stringlike clusters have been considered by Häkkinen et al.[47] when trying to elucidate positron trapping at jogs. They calculated a lifetime of a positron trapped in a row of six vacancies. The obtained value was equivalent to that for a single vacancy. Thus, a segmentation of the vacancy strings will not lead to a significant contribution of long-lived components. Besides, the lifetime spectra obtained gave no indication of long-lived components ≥ 250 ps (i.e., divacancies or spherical agglomerates) that would become evident even without a deconvolution procedure.

3. The interpretation of the threshold

The mean diffusion length L_+ of thermalized positrons in copper can be calculated from $L_+ = \sqrt{6D_+/\overline{\lambda}_f}$, where D_+ denotes the diffusivity and $1/\overline{\lambda}_f$ the mean lifetime of positrons in defect-free copper. The values for the diffusivity D_+ at room temperature, as reported in the literature, are scattered over the range of 0.3–0.7×10^{-4} m^2/s,[9] 0.9×10^{-4} m^2/s,[3] and 1.7×10^{-4} m^2/s.[69] Using $D_+ = 1 \times 10^{-4}$ m^2/s as a reasonable mean value and a mean positron lifetime of 110 ps,[70] $L_+ \approx 0.25$ μm is obtained. Thus, we can write the critical dislocation spacing as $d_c \approx 0.5$ μm $\approx 2L_+$. Consequently, the mean spherical volume that can be probed by a diffusing positron that thermalizes at maximum distance from a dislocation, i.e., just in the middle between two dislocations, is large enough that all positrons have a chance to reach a dislocation. This may serve as a rule of thumb for the sensitivity of positrons to dislocations at room temperature. It implies that the combined effect of trapping and detrapping of positrons along dislocation lines results in a rather small net trapping rate. Further temperature-dependent measurements expanding to low temperatures will be necessary for quantitative investigations.

Although several investigations of positron annihilation on plastically deformed metals have been described in the literature,[6,7,10,28,31,71–73] a sensitivity limit to plastic deformation has not yet been reported. McKee et al.[6] have performed positron lifetime measurements on copper single crystals after tensile deformation in the [110] direction at room tem-

perature. In Fig. 1 of Ref. 6 the mean positron lifetime starts to increase if a dislocation density in the range of 1×10^{12} to 3×10^{12} m^{-2} is exceeded. Dauwe *et al.*[31] concluded from their lifetime and line-shape measurements on cold-rolled polycrystalline copper specimens that below a dislocation density of 2×10^{12} m^{-2} the crystals appeared to be defect free for positrons. They emphasized that due to the dissipated energy during cold rolling, vacancies were already annealed and did not play a role in their treatment. These values agree well with our sensitivity limit of about 3×10^{12} m^{-2}. The investigations of Dauwe *et al.*[31] and McKee *et al.*[6] relied on the sandwich technique, which limited the number of deformation stages that could be investigated. A sensitivity threshold could not be extrapolated from the few available data. Dlubek *et al.*[74] reported that significant positron trapping sets in above a dislocation density of 10^{12} m^{-2}. This estimate is presumably based on an extrapolation of their angular correlation data obtained from a series of cold rolled Nickel polycrystals measured in sandwich geometry.

In irradiation experiments where the damage consists prevailingly in dislocation loops no threshold of positron annihilation data has been observed with respect to the loop density. This may be due to three main reasons. First, the dislocation loops are formed by irradiation induced vacancies or interstitials which are produced homogeneously distributed in the irradiated volume. Consequently, TEM observations also show a homogeneous distribution of small dislocation loops with separations in the range of a few nanometers up to about 0.1 μm depending on the irradiation dose and temperature (e.g., Ref. 75). These dislocation lines are much more homogeneously distributed than the long, extended dislocation lines produced during the early stages of plastic deformation. Thus, the probability of a positron to find a dislocation line on its random walk is higher in this case. Secondly, the loop density reported, e.g., by Urban[75] in copper irradiated with 650 keV electrons at 55 K is between 5 and 50×10^{15} cm^{-3}. Assuming 1 nm as the typical loop diameter this corresponds to a dislocation density between 3×10^{13} and 3×10^{14} m^{-2} which is already well above the sensitivity limit in plastic deformation. Moreover, those vacancies which form small spherical clusters and remain invisible for TEM will also contribute to a significant increase in positron lifetime.

B. Cyclic deformation

In order to illustrate the difficulties in understanding the positron annihilation measurements performed during fatigue, the next section briefly summarizes the characteristic microstructural features. We confine ourselves to face-centered cubic (fcc) materials under primary glide conditions in the state of cyclic saturation which is mechanically characterized by constant amplitudes of stress and strain and a constant shape for the hysteresis loops. For a more comprehensive presentation of fatigue microstructures, the reader is referred to some recent reviews by Laird *et al.*,[17] Basinski and Basinski,[18] and recent investigations of the microstructural evolution by Holzwarth and Eßmann[76,77]

In searching for an explanation of the experimental findings in Sec. IV B 2, it is important to keep in mind that the

FIG. 9. Typical microstructure for a copper single crystal fatigued well into cyclic saturation at room temperature at $\hat{\gamma}_{pl} \approx 4 \times 10^{-3}$. The stress amplitude at saturation is $\hat{\tau} = 28$ MPa. The micrograph is taken from a foil cut perpendicular to the primary edge dislocation lines $[(1\bar{2}1)$ section]. The ladderlike structure of persistent slip bands with its rather regularly spaced dislocation walls is clearly discernible from the surrounding matrix structure with their amoeboid shaped dislocation-dense *veins* and dislocation-poor *channels*. The orientation of the ladderlike PSB's matches exactly the direction of the primary Burgersvector. [Diffraction vector $\vec{g} = (20\bar{2})$.]

microstructure in cyclic saturation as described in Sec. IV B 1 is not yet established. In particular, the densities of dislocations and atomic defects are lower than those given below and steady state conditions preserving constant defect densities do not yet exist in the early stages of fatigue with resolved shear stress amplitudes of around 8 MPa. The structure, which is typical at the threshold stress, will undergo several rearrangements before reaching cyclic saturation. Nevertheless, the principal complexity of the defect spectra will be as outlined in Sec IV B 1.

1. The complexity of the fatigue defect spectra

We have seen in Sec. IV A that the correct description of the density and distribution of dislocations and atomic defects is essential for a correct interpretation of the positron-annihilation measurements. For the case of fatigue, the interpretation on the basis of an average dislocation density will be misleading in view of ordered dislocation arrangements such as those presented in Fig. 9. The highly ordered ladderlike structure of persistent slip bands (PSB's) is clearly dis-

cernible from the *matrix* structure consisting of amoeboid shaped dense *veins* and dislocation poor *channels*. PSB's consist of rather regularly spaced dislocation *walls* with dislocation densities of about 5×10^{15} m^{-2}, separated by channels with much lower dislocation densities of around 1×10^{13} m^{-2}. The dislocation densities in the veins and channels of the matrix structure are typically 10^{15} m^{-2} and 2×10^{12} m^{-2}, respectively. In the dense veins and walls, the primary edge dislocations are arranged in dipoles. In the channels, mainly screw dislocations and debris from dislocation reactions are present.

During cyclic saturation, nearly the whole applied plastic strain amplitude is localized in the PSB's. Hence, the surrounding matrix may be regarded as a passive structure with negligible dislocation motion. The experimental findings can be described by intrinsic resolved plastic strain amplitudes of PSB's and matrix (Cu, 300 K: $\hat{\gamma}_{PSB} = 9 \times 10^{-3}$ and $\hat{\gamma}_{matrix} = 6.5 \times 10^{-5}$). The volume fractions of PSB's (f) and matrix ($1-f$) are adjusted by the crystal in order to accomplish the applied plastic strain amplitude $\hat{\gamma}_{pl}$ after Winter's rule[78] $\hat{\gamma}_{pl} = (1-f)\hat{\gamma}_{matrix} + f\hat{\gamma}_{PSB}$ (see Refs. 18, 76, and 77, and citations there). A dynamic equilibrium between dislocation production and annihilation maintains a constant dislocation density in the PSB's whereas in the passive matrix structure a static situation prevails which preserves the defect spectra in the state as reached at the moment of phase separation into plastically active and passive areas.[76] Besides the dynamic equilibrium of dislocation production and annihilation, the crystal also adjusts to a dynamic equilibrium between the production and annihilation of atomic defects, a fact concluded from electrical resistivity measurements. The highest concentrations of atomic defects are established in the PSB walls by the annihilation of primary edge dislocations. If a primary edge dislocation enters a wall (or a vein), it will most probably react with a dipole thereby producing a new, more stable dipole with a smaller distance between the glide planes of the involved dislocations. If this new distance is smaller than ⩽1.6 nm (in copper),[23,83] the dipole will collapse thereby producing large local concentrations of atomic defects. This process is the main source of atomic defect production in PSB's.

The high concentrations of atomic defects favor the formation of clusters of various sizes and shapes or the condensation of vacancies as Frank dislocation loops. Clusters and Frank loops have been observed by TEM and are preferentially located in the dislocation dense areas.[24,25] Spherical clusters, which are invisible to TEM, give rise to a long-lived component in the positron-lifetime spectra.[25–27,81] The lifetimes and their respective intensities given in the literature vary appreciably. Values between 200 ps and over 350 ps are reported.[26,27]

Grobstein *et al.*[27] investigated the fatigue of nickel which had been irradiated with 47 MeV protons in order to produce ^{58}Co as an internal positron source. Although limited to nickel and its alloys, this *in situ* method represents a powerful tool in the aquisition of data from microstructural evolution processes. Their fatigue experiments yield positron-lifetime spectra with two lifetime components. The short lived component around 100 ps is attributed to annihilation in the perfect lattice or in the dislocations. The intensity of the longer-lived component increases with increasing num-

ber of deformation cycles whereas its value decreases from about 300 ps after 10 cycles to about 200 ps after 10 000 cycles (load control, $\hat{\tau} = 154$ MPa). This component is attributed to vacancy clusters of various sizes that undergo a size refinement with progressive fatigue. A refinement of microvoids during fatigue of copper was also reported by Lepistö *et al.*[26] which seems to depend on the crystal orientation and the loading history.

Since the definition of sensitivity to a certain type of defect requires a precise knowledge of the density and distribution of all defect types present, it is not possible to derive a sensitivity threshold for a certain defect type from fatigue investigations. Thus, another explanation for the threshold stress observed in fatigue has to be found.

2. The interpretation of the fatigue threshold—a two-phase system approach

The work of Basinski *et al.*[19] and Hancock and Grosskreutz[20] shows that the dislocation distribution becomes inhomogeneous during the early stages of fatigue, at resolved shear stress amplitudes of less than 4 MPa. By comparison with our mechanical data ($\gamma_{cum} \approx 1$ and $\hat{\tau} \approx 8$ MPa) and with the aid of the recorded cyclic hardening curve, the literature has been searched for a dislocation arrangement that most resembles that, present in our fatigued copper crystals. Basinski *et al.*[19] report that the inhomogeneous dislocation distribution that is most similar to ours is characterized by dislocation-dense regions with a local density of 5×10^{14} m^{-2} occupying 7% of the volume and dislocation-poor regions with an average density of 1×10^{11} m^{-2} in 93% of the volume.

In this case, it is possible to tentatively treat positrons, which thermalize in the nearly dislocation-free areas ($\varrho_{local} < \varrho_c$), as positrons in the perfect lattice. On the other hand, positrons which thermalize in the dislocation-dense regions will probably be unable to leave such regions due to the high density of traps. Consequently, dense regions may be considered as regions of saturation trapping. The assumption of saturation trapping is corroborated by, local *S*-parameter measurements with a positron microbeam in an area where exclusively PSB's are present.[82] Accordingly, two distinct mean lifetimes $1/\bar{\lambda}_{dense}$ and $1/\bar{\lambda}_{poor}$ may be attributed to the dislocation dense and poor regions, respectively. In order to check the plausibility of the threshold stress in fatigue we may estimate the mean positron lifetime from $1/\bar{\lambda}_{dense}$ and $1/\bar{\lambda}_{poor}$ weighted by the volume fractions of 0.07 and 0.93, respectively.[19] For this purpose we may identify $1/\bar{\lambda}_{poor}$ with the measured lifetime before deformation of about 130 ps $1/\bar{\lambda}_{dense}$ is much more difficult to assess and we will make use of the well defined microstructure in cyclic saturation.

A look at Fig. 9 may be helpful in illustrating PSB properties. The data hold for room temperature fatigue. The volume fractions occupied by PSB's and the matrix structure depend on the amplitude of the resolved plastic strain $\hat{\gamma}_{pl}$ (e.g., Refs. 18 and 77). At $\hat{\gamma}_{pl} = 4 \times 10^{-3}$, which is the maximum amplitude in our experiments, about 40% of the volume is occupied by PSB's and 60% by the matrix structure.[77] In the matrix structure one half of the volume is occupied by veins.[18,77] In the PSB's the volume fraction of the dense regions can be calculated from the mean wall thickness [0.1

μm (Ref. 77)] and the average wall spacing [1.4 μm (Ref. 77)]. With these data we can estimate that the mean positron lifetime measured in a specimen in cyclic saturation at $\hat{\gamma}_{\mathrm{pl}} = 4 \times 10^{-3}$ of 170 ps comprises as $0.34 \times 1/\overline{\lambda}_{\mathrm{dense}} + 0.66 \times 1/\overline{\lambda}_{\mathrm{poor}}$. Using $1/\overline{\lambda}_{\mathrm{poor}} \approx 130$ ps, we obtain $1/\overline{\lambda}_{\mathrm{dense}} \approx 240$ ps. This value has to be considered as an upper estimate since the dislocation poor regions can certainly not be treated as defect-free in cyclic saturation. The density of dislocations and dislocation debris in the dislocation-poor channels in the PSB are certainly well above the detection limit for positrons. Nevertheless, our estimate of 240 ps indicates that in the dense regions microvoids and spherical vacancy clusters may be present.

Using the volume fractions of dense and poor regions in the early stages of fatigue of 0.07 and 0.93 and the mean lifetimes of 240 and 130 ps, respectively, we may expect a mean positron lifetime of 138 ps at our sensitivity threshold. This value is in fair agreement with our measurements at the sensitivity threshold of $\hat{\tau} = (8 \pm 1)$ MPa. Thus, the sensitivity limit in fatigue may at least tentatively be explained by the inhomogeneous dislocation arrangement and the formation of vacancy clusters.

C. Interpretation of annealing experiments

Striking differences in the annealing behavior of tensile and fatigue specimens were observed. While the annealing of vacancies was completed after 1 h at 450 K in the tensile specimen deformed to $\gamma = 50\%$, pronounced annealing was observable only after a second annealing stage at 550 K in the fatigue specimen. Furthermore, the retained increase of positron lifetime after the final annealing stage shows a remarkable resistance to the fatigue defect spectra. In particular, 65% of the increase of positron lifetime was retained after the two stage annealing of the fatigue specimen whereas 50% easily annealed out in the tensile specimen already after the first annealing stage at 450 K.

The observed annealing resistance of the fatigued specimen coincides qualitatively with investigations by Kupca et al.[72] who observed that at least a temperature of 550 K was necessary for the onset of annealing. This is, however, inconsistent quantitatively with our results which show that annealing begins at about 450 K.

The annealing behavior of our tensile specimen agrees qualitatively with earlier investigations reported in the literature, e.g., with Kuribayashi et al. who found that 70% of the effect measured by angular correlation had been retained after single and divacancies were removed[29] Positron lifetime measurements after annealing of plastically deformed specimens were performed by Dauwe et al.,[31] Hinode et al.,[79] and Saimoto et al.[80] There are quantitative disagreements with respect to the onset of annealing and the retained increase in the mean positron lifetime between these examinations and ours, probably due to the different type and geometry of deformation. The conditions of deformation range from tensile experiments on single crystals oriented for multiple slip[80] to the frequently applied cold rolling of polycrystalline specimens.[31] Hinode et al.,[79] Saimoto et al.,[80] and Dauwe et al.[31] report the onset of recovery at 553, 573, and 653 K, respectively. Measurements performed after tensile deformation up to 41.4 MPa on crystals oriented for multiple slip[80]

(present case: single slip, 45 MPa) yielded an increase of 31 ps of the mean positron lifetime (present case: 16 ps); after 30 min of annealing at 573 K 19 ps were retained (present case: 8 ps after 60 min at 550 K). This different behavior indicates that the measured mean positron lifetimes depend strongly on the dislocation arrangement and the density and configuration of jogs on dislocations.

The different annealing behavior of tensile and fatigue specimens may be explained by different configurations of vacancy clusters, which are stringlike if they are produced by jog dragging[11–13] whereas spherical clusters are favored in fatigue when the annihilation of edge dislocations[23,83] creates high concentrations of atomic defects. Another process which might reduce the positron lifetime is the condensation of atomic defects in Frank loops which offer less open volume to the positrons than the same number of vacancies arranged as a spherical cluster. From this comparison we conclude, on the other hand, that multiple slip and the conditions in cold rolling cause high supersaturations of vacancies which enable the formation of spherical clusters.

Further experiments are necessary to obtain experimental data on the annealing behavior of vacancies as a function of the plastic strain γ_{pl}. A calculation of the vacancy concentration and the dislocation density according to Eqs. (2) and (1) yields $C_V = 3 \times 10^{-5}$ and $\varrho = 6.5 \times 10^{13}$ m^{-2} after tensile deformation up to 43.5 MPa. By comparing these figures with those obtained at 10 MPa in Sec IV A, it is evident that the vacancy concentration rises much more sharply than the dislocation density. One may speculate that the probability of jog formation increases with dislocation density which is, on the other hand, a prerequisite for the production of atomic defects. Systematic tensile deformation experiments for different values of γ_{pl} and subsequent annealing treatments may therefore provide information on the formation processes of atomic defects. Combined with electrical resistivity measurements, which are also sensitive to interstitials, biases in the production of vacancies and interstitials might be accessible which are sometimes discussed in the literature (e.g., Ref. 83).

D. Positron trapping at dislocations

In the preceding sections, dislocations were treated as one-dimensional entities capable of trapping positrons at room temperature and details of the trapping process and the positron annihilation were not regarded (see the actual state of knowledge outlined in Sec. I). This scenario is supported by the interpretation of the observed threshold stress in tensile deformation as a sensitivity limit of positron annihilation to dislocations.

1. Vacancies and jogs

The experimental findings do not permit conclusions to be drawn about the annihilation sites of the positrons, however, we would like to comment on the *vacancies associated with dislocations* which are frequently mentioned in the literature.

Our first point is based on molecular dynamic calculations on the mechanisms of pipe diffusion, i.e., the enhanced self-diffusion along dislocation lines (see the reviews by Baluffi and Granato[84] and Atkinson and Le Claire[85]). Recent calculations by Huang et al.[86,87] confirm that the formation energy

of a vacancy in the disturbed, disordered region around a dislocation line is only about 80% of the energy required to form a vacancy in the perfect lattice. This explains higher vacancy concentrations along dislocation lines. These vacancies are not free, they are elastically attracted by the stress field around a dislocation line and their mobility is strongly reduced except for motion along the dislocation line. (A vacancy formed with reduced formation energy and the same migration energy as in the bulk would violate the basic laws of thermodynamics.) The elastic interaction between vacancies and dislocations in cubic metals is extremely weak. Elasticity theory only explains a slightly higher concentration of vacancies in the compressive zone around an edge dislocation.[42] If the elastic energy stored at the site of vacancy formation is taken into account, one obtains a lower formation energy, a higher attraction and, consequently, a higher vacancy concentration. The radius of this dislocation core with increased vacancy concentration may be about 0.5 nm.[42,84,87] These arguments may also account for a significant vacancy concentration around a screw dislocation as it is also surrounded by a stress field. From this point of view, deep traps for positrons should be present along both edge and screw dislocation lines. It is not therefore *a priori* clear why edge and screw dislocations should be discernible by positrons as stated by Park *et al.*[88] This might explain the findings of Hidalgo *et al.*[5] who did not observe such a difference in iron samples deformed at 77 K which prevailingly contained screw dislocations.

The calculations of Huang *et al.*[86] also indicate that the region of lattice disorder where vacancy formation is facilitated may extend into the stacking fault ribbon which expands between the partials of dissociated edge dislocations. As screw dislocations may also dissociate, this feature would result in a similar trapping behavior of edge and screw dislocations.

If jogs act as positron traps, only small jogs have to be considered, as being created by intersection processes of dislocations or by vacancies attached to a dislocation. A vacancy on an idealized perfect edge dislocation would be equivalent to a jog-antijog pair separated by one atomic distance. A further vacancy migrating to the dislocation line may either produce a further jog-antijog pair thereby increasing the jog density on the dislocation line or it may increase the separation of the existing jog pair leaving the jog density constant. Thus, the annealing of vacancies by migration to dislocations acting as vacancy sinks does not necessarily increase the jog density—the same considerations hold for interstitials which are mobile at much lower temperatures than vacancies. The lifetime of a positron trapped in a jog depends on the local density of the ion cores, i.e., its microstructure, which will be different for ideal (constricted) or dissociated (extended) jogs. Presently, it seems impossible to check these considerations experimentally.

In the dislocation walls of PSB's, the edge dislocations arranged in dipoles contain enormous densities of jogs which are produced as a consequence of the annihilation of screw dislocations encountered in the channels. These jogs are the cross slip traces of the screw dislocations and may be as high as 50 to 60 nm.[89,90] In TEM investigations on fatigued specimens whose dislocation arrangements had been fixed by subsequent irradiation with fast neutrons no screw dislocation

dipoles were observed with a spacing of less than 50 nm. From these findings it was concluded that narrower dipoles annihilate by cross slip.[89] It is conceiveable that such long jogs do not necessarily provide the same trapping properties as monoatomic jogs. They are probably seen as short secondary dislocation segments by the positrons. So far, no attention has been paid to these microstructural features.

2. Dependence on the modulus of the Burgers vector

According to the best of the authors knowledge, only one systematic investigation on the size of the Burgers vector was performed by Shirai *et al.*[91] The measurements were carried out at room temperature on a variety of materials and after a variety of treatments, including plastic deformation, quenching, and irradiation in order to produce glide dislocations, and partial dislocations which border prismatic dislocation loops and stacking fault tetrahedra. Indeed, a linear increase in the positron lifetime and the modulus of the Burgers vector was observed. Nevertheless, the investigated partial dislocations are rather short segments and do not typify the situation occurring during plastic deformation.

V. SUMMARY AND CONCLUSIONS

The β^{+}-γ-coincidence spectrometer enables *in situ* positron lifetime measurements to be performed, which permit the observation of microstructural evolution during plastic deformation in fine steps. It has been observed that a threshold stress has to be exceeded before plastic deformation is detectable by positron annihilation. The threshold stresses are (10 ± 1) and (8 ± 1) MPa for tensile deformation and fatigue, respectively. For tensile straining a sensitivity threshold of positron annihilation to homogeneously distributed dislocations could be derived which corresponds to a critical dislocation density of $(3\pm1)\times10^{12}$ m^{-2}. Due to the large number of measurements permitted by the *in situ* technique, at least for tensile straining, it could be demonstrated that the positron lifetime shows a linear increase with increasing resolved shear stress above the threshold. Up to 43.5 MPa no saturation was observed. In fatigue the positron lifetime starts to saturate at a resolved plastic shear stress amplitude of about 25 MPa.

A precise knowledge of the types of defects, their concentrations, and their spatial distributions turned out to be essential for the interpretation of the positron-annihilation measurements. The sensitivity limit to dislocations could be obtained because dislocations are homogeneously distributed and a disturbing effect of vacancies could be ruled out due to their low concentration and their inhomogeneous spatial distribution. This approximates a nearly ideal situation.

The microstructures observed in the early stages of fatigue are much more complex than the respective ones observed during tensile testing. We tentatively simplified the situation by considering two different phases, one with a high density of dislocations, vacancies, and vacancy clusters of different sizes and shapes and a second one with a much lower dislocation density and less vacancy clusters. The two phases are supposed to exhibit different mean positron lifetimes. The first phase will probably exhibit the longest mean lifetime which can be observed in a deformed metal. Such a model may have some advantages in evaluating microstruc-

tural evolution processes by positron annihilation. It is intended to apply a positron microbeam with a diameter in the micron range[82] to study the two phases separately and to elucidate the local distribution of positron traps. The microbeam will help to check whether this simplification is justified and useful.

The comparison of positron lifetime changes in tensile and cyclic deformation shows that the same lifetime changes with respect to the undeformed state were obtained from specimens containing different average dislocation densities. The critical dislocation density at the sensitivity threshold in tensile deformation was obtained as $(3\pm1)\times10^{12}$ m^{-2}. In fatigue experiments one has to deal with an inhomogeneous distribution with an average density of 3.5×10^{13} m^{-2} at the sensitivity threshold. Obviously, the clustering of dislocation in small areas with extremely high dislocation density hinders a detection in an earlier stage of fatigue with lower dislocation density such as the one detectable in tensile tests. For any attempt to determine the dislocation density from positron lifetime measurements a precise knowledge on the deformation history is essential. This conclusion is emphasized by our multiple step test which give different values for the increase of positron lifetime per stress increment depending on the applied resolved plastic strain amplitude.

[1] R. N. West, Adv. Phys. **22**, 263 (1973).

[2] A. Seeger, J. Phys. F **3**, 248 (1973).

[3] P. J. Schulz and K. G. Lynn, Rev. Mod. Phys. **60**, 701 (1988).

[4] G. Trumpy, Phys. Lett. A **192**, 261 (1994).

[5] C. Hidalgo, G. González-Doncel, S. Linderoth, and J. San Juan, Phys. Rev. B **45**, 7017 (1992).

[6] B. T. A. McKee, S. Saimoto, A. T. Stewart, and M. J. Stott, Can. J. Phys. **52**, 759 (1974).

[7] J. Baram and M. Rosen, Phys. Status Solidi A **16**, 263 (1973).

[8] J. G. Byrne, in *Dislocations in Solids*, edited by F. R. N. Nabarro (North-Holland, Amsterdam, 1983), Vol. 6, pp. 263.

[9] R. M. Nieminen and M. J. Manninen, in *Positrons in Solids*, edited by P. Hautojärvi, *Topics in Current Physics*, Vol. 12 (Springer-Verlag, Berlin, 1979), p. 143.

[10] K. Petersen, I. A. Repin, and G. Trumpy, J. Phys.: Condens. Matter **8**, 2815 (1996).

[11] A. Seeger, Philos. Mag. **46**, 1194 (1955).

[12] P. B. Hirsch and D. H. Warrington, Philos. Mag. **6**, 735 (1961).

[13] P. B. Hirsch, Philos. Mag. **7**, 67 (1962).

[14] U. Eßmann, Phys. Status Solidi **12**, 707 (1965); **12**, 723 (1965).

[15] U. Eßmann, Phys. Status Solidi **17**, 725 (1966).

[16] H. Mughrabi, in *Constitutive Equations in Plasticity*, edited by A. S. Argon (MIT Press, Cambridge, MA, 1975), p. 199.

[17] C. Laird, P. Charsley, and H. Mughrabi, Mater. Sci. Eng. **81**, 433 (1986).

[18] Z. S. Basinski and S. J. Basinski, Prog. Mater. Sci. **36**, 89 (1992).

[19] S. J. Basinski, Z. S. Basinski, and A. Howie, Philos. Mag. **19**, 899 (1969).

[20] J. R. Hancock and J. R. Grosskreutz, Acta Metall. **17**, 77 (1969).

[21] J. C. Grosskreutz and H. Mughrabi, in *Constitutive Equations in Plasticity*, edited by A. S. Argon (MIT Press, Cambridge, MA, 1975), p. 251.

[22] C. Corbel, M. J. Puska, and R. M. Nieminen, in *Positron Annihilation*, edited by P. C. Jain, R. M. Singru, and K. P. Gopinathan (World Scientific, Singapore, 1985), p. 576.

[23] U. Eßmann and H. Mughrabi, Philos. Mag. A **40**, 731 (1979).

[24] J. Piqueras, J. C. Grosskreutz, and W. Frank, Phys. Status Solidi A **11**, 567 (1972).

[25] L. Díaz, R. Pareja, M. A. Pedrosa, and R. Gonzáles, Phys. Status Solidi A **92**, 159 (1985).

[26] T. K. Lepistö, H. Huomo, V.-T. Kuokkala, P. Hautojärvi, and P. O. Kettunen, in *Proceedings of the 9th International Conference on the Strength of Metals and Alloys*, Haifa, Israel, July 1991, edited by D. G. Brandon, R. Chaim, and A. Rosen (Freund, London, 1991), p. 545.

[27] T. L. Grobstein, S. Sivashankaran, G. Welsch, N. Panigrahi, J. D. McGervey, and J. W. Blue, Mater. Sci. Eng. A **138**, 191 (1991).

[28] S. Dannefaer, D. P. Kerr, S. Kupca, B. G. Hogg, J. U. Madsen, and R. M. Cotterill, Can. J. Phys. **58**, 270 (1980).

[29] K. Kuribayashi, S. Tanigawa, S. Nanao, and M. Doyama, Phys. Lett. **40A**, 27 (1972).

[30] E. Hashimoto, T. Shiraishi, N. Kamigaki, and T. Kino, J. Phys. Soc. Jpn. **57**, 3233 (1988).

[31] C. Dauwe, M. Dorikens, L. Dorikens-Vanpraet, and D. Seegers, Appl. Phys. **5**, 117 (1974).

[32] M. Doyama and R. M. Cotterill (unpublished).

[33] G. Dlubek, O. Brümmer, and E. Hensel, Phys. Status Solidi A **34**, 737 (1976).

[34] M. L. Johnson, S. F. Saterlie, and J. G. Byrne, Metall. Trans. A **9**, 841 (1978).

[35] S. Mantl and W. Triftshäuser, Phys. Rev. B **17**, 1645 (1978).

[36] G. M. Hood and B. T. A. McKee, J. Phys. F **8**, 1457 (1978).

[37] E. Hashimoto and T. Kino, J. Phys. Soc. Jpn. **60**, 3167 (1991).

[38] E. Hashimoto, M. Iwami, and Y. Ueda, J. Phys.: Condens. Matter **6**, 1611 (1994).

[39] E. Hashimoto, J. Phys. Soc. Jpn. **62**, 552 (1993).

[40] C. Hidalgo and S. Linderoth, J. Phys. F **18**, L263 (1988).

[41] S. Mäkinen, H. Häkkinen, and M. Manninen, Phys. Scr. **T33**, 206 (1990).

[42] See, e.g., J. P. Hirth and J. Lothe, *Theory of Dislocations* (Wiley, New York, 1982); F. R. N. Nabarro, *The Theory of Crystal Dislocations* (Oxford University Press, Oxford, 1967).

[43] V. M. Chernov and M. M. Savin, Phys. Status Solidi A **47**, 45 (1978).

[44] C. H. Hodges and M. J. Stott, Solid State Commun. **12**, 1153 (1973).

[45] C. H. Hodges, Phys. Rev. Lett. **25**, 284 (1970).

[46] J. Arponen, P. Hautojärvi, R. Nieminen, and E. Pajanne, J. Phys. F **3**, 2092 (1973).

[47] H. Häkkinen, S. Mäkinen, and M. Manninen, Phys. Rev. B **41**, 12 441 (1990).

[48] J. W. Martin and R. Paetsch, J. Phys. F **2**, 997 (1972).

[49] S. C. Liu, B. Wang, X. H. Li, and S. J. Wang, Mater. Sci. Forum **105-110**, 1133 (1992).

[50] E. Kuramoto, V. Novák, and V. Paidar, Scr. Metall. Mater. **26**, 557 (1992).

[51] D. Hoeckelman and H. P. Leighly, Jr., Phys. Status Solidi A **138**, 147 (1993).

[52] D. Hoeckelman and H. P. Leighly, Jr., Phys. Status Solidi A **149**, K19 (1995).

[53] C. Q. Tang, Z. H. Shi, and X. Z. Li, Phys. Status Solidi A **137**, K5 (1993).

[54] R. Rajaraman, P. Gopalan, B. Viswanathan, and S. Venkadesan, J. Nucl. Mater. **217**, 325 (1994).

[55] S. Hansen, U. Holzwarth, M. Tongbhoyai, T. Wider, and K. Maier, Appl. Phys. A: Solids Surf. **65**, 47 (1997).

[56] Stack of piezoelectric elements P-239.180 supplied by PI-Physik Instrumente D-76337 Waldbronn, Germany.

[57] Capacitive Sensor D-100.00 supplied by PI-Physik Instrumente D-76337 Waldbronn, Germany.

[58] U. Holzwarth and P. Hähner, Philos. Mag. A **72**, 691 (1995).

[59] R. Berner and H. Kronmüller, in *Moderne Probleme der Metallphysik*, edited by A. Seeger (Springer-Verlag, Berlin, 1965), Vol. 1, p. 35.

[60] J. Morrow, in *Internal Friction Damping and Plasticity* (American Society of Testing and Materials, Philadelphia, 1964), Vol. 378, p. 45.

[61] J. G. Sevillano, in *Materials Science and Technology*, edited by R. W. Cahn, P. Haasen, and E. J. Kramer (VCH, Weinheim, 1993), Vol. 6, p. 19.

[62] G. Saada, Acta Metall. **9**, 166 (1961); **9**, 965 (1961).

[63] F. R. N. Nabarro, Z. S. Basinski, and D. B. Holt, Adv. Phys. **13**, 193 (1964).

[64] P. Coulomb, Scr. Metall. **15**, 769 (1981).

[65] G. Simmons and H. Wang, *Single Crystal Elastic Constants and Calculated Aggregate Properties*, 2nd ed. (MIT Press, Cambridge, MA, 1971).

[66] A. van den Beukel, in *Vacancies and Interstitials in Metals*, edited by A. Seeger, D. Schumacher, W. Schilling, and J. Diehl (North-Holland, Amsterdam, 1970), p. 427.

[67] P. Hautojärvi, J. Heinö, M. Manninen, and R. Nieminen, Philos. Mag. **35**, 973 (1977).

[68] P. Alexopoulos and J. G. Byrne, Metall. Trans. A **9**, 1829 (1978).

[69] E. Soininen, H. Huomo, P. A. Huttunen, J. Mäkinen, A. Vehanen,

and P. Hautojärvi, Phys. Rev. B **41**, 6227 (1991).

[70] H.-E. Schaefer, W. Stuck, F. Banhart, and W. Bauer, in *Vacancies and Interstitials in Metals and Alloys*, edited by C. Abromeit and H. Wollenberger (Trans Tech, Aedermannsdorf, 1987), p. 117.

[71] M. Iwami, E. Hashimoto, and Y. Ueda, J. Phys.: Condens. Matter **7**, 9935 (1995).

[72] S. Kupca, D. P. Kerr, B. G. Hogg, and Z. S. Basinski, Can. J. Phys. **60**, 201 (1982).

[73] L. P. Karjalainen, M. Moilanen, R. Myllylä, and K. Palomäki, Phys. Status Solidi A **62**, 597 (1980).

[74] G. Dlubek, O. Brümmer, and P. Sickert, Krist. Tech. **12**, 295 (1977).

[75] K. Urban (unpublished).

[76] U. Holzwarth and U. Eßmann, Appl. Phys. A: Solids Surf. **57**, 131 (1993).

[77] U. Holzwarth and U. Eßmann, Appl. Phys. A: Solids Surf. **58**, 197 (1994).

[78] A. T. Winter, Philos. Mag. **30**, 719 (1974).

[79] K. Hinode, S. Tanigawa, and M. Doyama, J. Phys. Soc. Jpn. **41**, 2037 (1976).

[80] S. Saimoto, B. T. A. McKee, and A. T. Stewart, Phys. Status Solidi A **21**, 623 (1974).

[81] P. O. Kettunen, T. Lepistö, G. Kostorz, and G. Göltz, Acta Metall. **29**, 969 (1981).

[82] H. Greif, M. Haaks, U. Holzwarth, U. Männig, M. Tongbhoyai, K. Maier, J. Bihr, and B. Huber, Appl. Phys. Lett. **71**, 1 (1997).

[83] U. Essmann, U. Gösele, and H. Mughrabi, Philos. Mag. A **44**, 405 (1981).

[84] R. W. Baluffi and A. V. Granato, in *Dislocations in Solids*, edited by F. R. N. Nabarro (North-Holland, Amsterdam, 1979), Vol. 4, p. 13.

[85] A. Atkinson and A. D. Le Claire (unpublished).

[86] J. Huang, M. Meyer, and V. Pontikis, J. Phys. III **1**, 867 (1991).

[87] J. Huang, M. Meyer, and V. Pontikis, Phys. Rev. Lett. **63**, 628 (1989).

[88] Y.-K. Park, J. T. Waber, M. Meshii, C. L. Sneard, Jr., and C. G. Park, Phys. Rev. B **34**, 823 (1986).

[89] H. Mughrabi, F. Ackermann, and K. Herz, in *Fatigue Mechanisms*, edited by J. T. Fong (American Society for Testing and Materials, Philadelphia, 1979), Vol. 675, p. 69.

[90] J. Lèpinoux and L. P. Kubin, Philos. Mag. A **51**, 675 (1985).

[91] Y. Shirai, K. Matsumoto, G. Kawaguchi, and M. Yamaguchi, Mater. Sci. Forum **105-110**, 1225 (1992).